*34th EPS Conference on Plasma Phys. Warsaw, 2 - 6 July 2007 ECA Vol.**31F**, P-1.153 (2007)*

Plasma Edge Dynamics during Alfvén Wave Injection into TCABR Plasmas

C.Ribeiro*, V.Bellintani, A.G.Elfimov, J.I.Elizondo, A.N.Fagundes, R.M.O.Galvão, T.M.Germano, Yu K. Kuznetsov, I.C.Nascimento, E.M.Ozono, L.F.Ruchko, W.P.de Sá, E.K.Sanada, J.H.Severo, †C.Silva, O.C.Usuriaga *celso_ribeiro@hotmail.com

Institute of Physics, University of São Paulo, São Paulo, SP, Brazil.
†Associação EURATOM/IST, Centro de Fusão Nuclear, Lisboa, Portugal

Introduction

Alfvén Waves (AW)[1] is considered an attractive scheme for heating[2], current drive (CD) and as a tool for creating transport barriers via induced plasma flow in a tokamak plasmas[3]. The AW heating scheme is based on the mode conversion of the RF field induced by an antenna into a kinetic AW, which ultimately heats the electrons. This conversion is a local resonant process[2].

The aim of the present work is to present preliminary results on a clear signature of particle confinement improvement in moderated target density, reactor relevant plasmas driven by a relatively rather low AW power injected in TCABR. Analysis on the edge physics in this scenario is presented.

Hardware and Experiment

Alfvén waves (AW) are being regularly launched into TCABR tokamak [R=0.615m, a=0.18m, Ip≤120kA, ne(bar)≤$4x10^{19}m^{-3}$, Te(0)≤600eV, Ti(0)≤400eV, discharge duration of 100ms, approximately, and solid circular poloidal divertor]. The basic pressure is around $4x10^{-7}$mbar prior conditioning by the Taylor cleaning method.

Alfvén wave antenna has a single module, with two straps, so that a broad spectrum of modes can be excited. In particular, for the present conditions, modes with both poloidal numbers M=+1/-1 are expected to be simultaneously excited. The Alfvén wave frequency is ≈4MHz with a power of ≈30kW, i.e. approximately only 16% of the Ohmic power (V_LIp ≈187kW).

A versatile triple Langmuir probe was commissioned for edge studies. Electron temperature (Te), plasma floating and potential (Vf and Vp), radial electric field (Er) and plasma density (ne), as well as their fluctuations, were directly measured or inferred. The probe is vertically placed on the top of the vessel at the position of the geometric radius (R). It is composed of 4 tungsten tips, 3mm length and 0.92mm diameter. They are 5mm equally spaced from any tip to the opposite. The tips are aligned with respect to the total magnetic at in such way that 2 tips just avoid the field shadow effect and the other two are near the poloidal field direction. The first pair measured the ion saturation current (I_{si}) and the second the floating potentials (V_{f1} and V_{f2}). The entire probe structure can rotate what allows a good alignment. Sample rate was 1MHz for all probe signals.

The experimental results reported here were obtained for hydrogen discharges with the following parameters Ip≈85kA, ne(bar)≈$1.8 \times 10^{19} m^{-3}$, V_L≈2.2, $B_T(0)$=1.15T, and q_ψ≈3.5.

Results

The basic signals are shown in fig.1. The black lines and the red lines here correspond to the discharge with and without AW injection, respectively.

When the AW are injected (fig1h), Ip (fig.1a) slightly increases from 85kA to a maximum 86kA (≈1.2%) in ≈1ms and maintain this ≈1kA for ≈2ms, with respect to a discharge without AW injection. Simultaneously, V_L (fig.1a) drops from 2.2 to 1.9V (minimum) in the same ≈1ms, but increases again to the expected value without AW injection in a scale of ≈2ms too. The overall effect of Ip increase and the V_L reduction lasts up to ≈3ms. This correlation between Ip and V_L is a clear sign of current drive. The CD efficiency is ≈0.033kA/kW, and the reason CD can not be maintained is not understood yet, but it might be related to the increase of the central density mainly. Therefore, in theory, 2.6MW could maintain this discharge if density control would be available.

The 2mm multi-chord interferometer signals are shown in the fig.1b. They are placed vertically at r/a=-0.1, 0.5, 0.8. The density at centre (r/a=-0.1), mid radius (r/a=0.5) and at the edge (r/a=0.8) delay 2, 1, and 1ms to rise, after the AW are applied. These densities keep increasing after the CD effect vanish until the times ≈85, 80, and 77ms, respectively, which are approximately the time in which the AW power starts to reduced rapidly (the RF signal in fig1h is the monitoring current flowing through the antennas straps, so the effective AW injected power varies with the square this parameter). The fact the central chords show much larger densities increase than the edge, i.e., 20%, 20% and 13%, respectively, at 80ms, indicates a much stepper ne profile over 0.5<r/a<0.8.

The central electron temperature Te(0) (fig1c) was calculated by a 1-D code for a cylindrical geometry, which simulates the toroidal field diffusion with the Spitzer resistivity[4]. It was obtained after an interactive matching between the experimental and the calculated V_L values. The Te(0) time resolution is ≈1ms. A small heating is obtained: Te(0).increases from ≈435 to ≈455eV (≈5%) in ≈3ms but it vanishes in the next ≈2ms.

Analysis of line radiation impurities (C, B, Cu) by spectroscopy shows that their concentrations do not increase with the AW injection. CIII and Hα monitors (fig.1d) show the first just increasing with central density but the second practically saturates after just $\approx$1ms. This suggests that there is no further recycling with the density rise, which is the sign of better particle retaining, i.e. particle confinement improvement.

The bolometer central chord (r/a$\approx$0) signal (fig.1c) increases with the central density but this extra radiative power losses might be negligible since the total stored energy increases with the AW injection (due to the density not to the temperature) as seem independently from the poloidal beta measured by the diamagnetic loop β_p(dia) (fig.1e) or calculated via equilibrium assumption β_p(equ) (fig.1f).

The changes in the density profile lead to an increase on the poloidal field fluctuations (Mirnov) activity as shown in the fig.1g. This is due to the increase on the amplitude of the low poloidal mode number m (fig2g in log10 scale). However, this increase on the Mirnov activity does not lead to major plasma MHD instabilities but to micro-instabilities as evidenced by the rise of the fluctuations amplitude on ne, Te, and Vp (fig2a/b/c, respectively). These signals were measured or inferred at the edge (r/a=1). Here ne $\propto$ Isi/Te½ and Vp=$\langle V_f \rangle$+2.6Te, where $\langle V_f \rangle = (V_{f1}+V_{f1})/2$.

The ne, Te, and Vp (fig2a/b/c, respectively) mean values do not vary substantially with the AW injection either here at r/a=1 or at the scrap-off layer (SOL). In particular, ne value increase $\approx$15% at 80ms. This is in agreement to the lower density increase of the line integral density measured closed to the edge (r/a=0.8).

In the fig2d the anomalous radial flux $\Gamma(neE_\theta)$ is shown. This parameter is due to the cross-correlation of ne and the poloidal electric (E_θ) field fluctuations. For simplicity here the Te contribution for E_θ is neglected, thus $E_\theta = -\nabla_\theta Vp \approx (V_{f1}-V_{f2})/d$, where is d is the distance between the 2 tips along the quasi-poloidal direction. The values of $\Gamma(neE_\theta)$ varies from $1x10^{20}m^{-2}s^{-1}$ at the time of AW injection to a maximum of $2.4x10^{20}m^{-2}s^{-1}$ at 88.5ms when it crashes to a negligible value. The increase of $\Gamma(neE_\theta)$ is due to the progressive better correlation Coe(neE_θ) (fig.2e) and a more favorable change (reduction) of the phase Pha(neE_θ) (fig.2f) between of ne and E_θ fluctuations. The crash might be the result of the Mirnov activity reduction below a threshold.

By using the Stangeby model for the natural particle loss[5] and the parameters of the present experimental condition, .it follows that $\Gamma(SOL) \approx 10x10^{20}m^{-2}s^{-1}$ which is more than 5 times the maximum anomalous flux, so the global transport is not substantially changed by the extra anomalous transport driven by AW injection, so the net effect still leads to a improved particle confinement scenario.

In order to explain the observed CD and the calculated heating effects, the AW absorption and the field structure are simulated using 2D ALTOK code[6]. For a 3.9MHz generator frequency and a $2.3\text{x}10^{19}\text{m}^{-3}$ central density for a parabolic profile with 0.8 power, (typical values for this kind of discharges) the absorption is absent. Even for 10% higher density, the global AW resonance stays out of the resonance condition. Taking into account the 2% impurity of C^{+3} or O^{+4} its found that the absorption is coming to be high for modes N/M=-3,-4/-1. In this case, ion-ion global AW resonance is formed in the plasma core limited by the C^{+3} cyclotron resonance zone which can explain the efficient plasma heating. This scheme is analogous to the minority ICR heating.

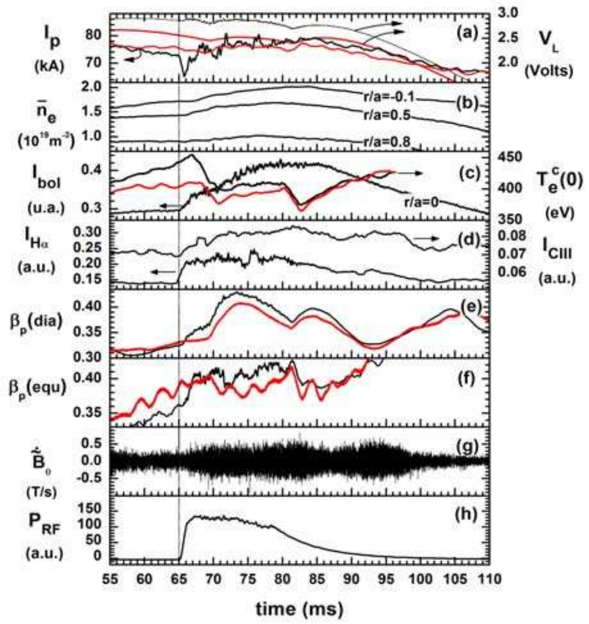

Fig. 1 Basic signals of a discharge with (black line) and without (red line) AW injection. See the text for the definitions.

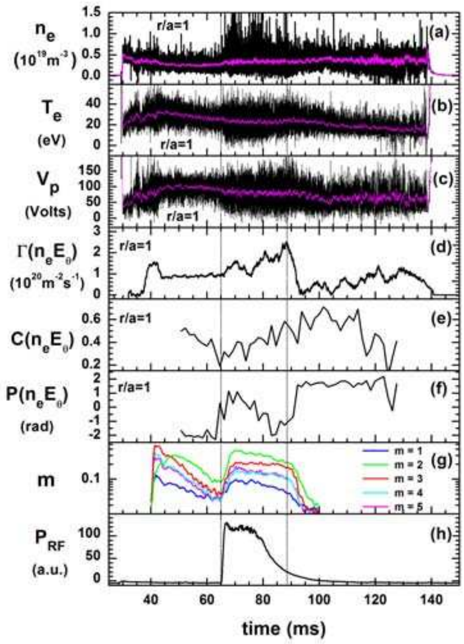

Fig. 2 Triple Langmuir probe signals for a similar discharge to that shown in Fig.1. The probe here was positioned right at the limiter (r/a=1). Se the text for the definitions

Acknowledgement: The main author partially supported by a fellowship from CNPq (Brazilian National Council for Scientific and Technological Development)

References

[1] H. Alfvén, Nature, 150, 450 (1942).
[2] J.Taronis and W. Grossman, Z. Phys. 261, 203 (1973).
[3] A.G.Elfimov et al, Plasma Phys and Control. Fusion, 40, 451 (1998).
[4] L. F. Ruchko *et al*., Brazilian Journal of Physics 32, 57 (2002).
[5] P. C. Stangeby and G. M. McCraken, Nucl. Fusion, 30, 1225 (1990).
[6] A. G. Elfimov *et al*, Brazilian Journal of Physics 32, 34 (2002)